Why is spray forming a rapid solidification process?

Warum ist Sprühkompaktieren ein Schnell-Erstarrungsprozess?

H. Henein

Since the invention of spray forming by Prof. Singer in the early 80's, many researchers have attempted to explain the rapid solidification features of the spray deposit through mathematical modelling of the process. The break-up of the stream into atomized drops followed by the deposition of these semi-solid droplets into a rotating deposit have been simulated using both the energy and the momentum equations. These models, however, do not explain the fineness of structure observed in spray formed products when compared to cast structures of similar dimensions and experiencing similar cooling rates. A single fluid technique provides an ideal tool to study the effect of atomization variables on the structure evolution of a spray formed deposit. It will be shown based on Cu-6Sn, Al-Cu and Al-Fe alloys that the undercooling of second and subsequent phases in the deposit accounts for the rapid solidified structure in spray forming.

Keywords: Spray forming / rapid solidification

Schlüsselwörter: Sprühkompaktieren / Schnell-Erstarrung

1 Introduction

Since the invention of spray forming by Prof. Singer in the early 80's, many researchers have attempted to explain the rapid solidification features of the spray deposit. As recently as 1995, Grant [1] published a review of Spray Forming. It was a very comprehensive review of the process involving the breakup of a liquid metal stream using gas atomization, followed by the collection of semi-solid droplets onto a rotating substrate. A number of important features are discussed including the state of understanding of atomization, droplet dynamics and thermal history as well as droplet deposition and deposit solidification. It is clearly shown that one of the outcomes of this process is a very fine scale microstructure, low levels of segregation, fine precipitates, extended solid solubility and depending on the alloy system, the presence of metastable phases. To explain these outcomes, researchers have modelled the spray forming process using heat and momentum equations for two phase flows. The resultant cooling rates in the deposit have been estimated to be slightly higher than of an ingot of similar dimension but produced using traditional pour and cast techniques. In fact, the high deposition rate of droplets in spray forming coupled with the continued solidification of these droplets, appear to have resulted in some remelting of solid that had formed in the droplet prior to deposition. It has also been postulated that the fine structure of the deposit is attributed to the break-up of dendrites in the droplets as they land on the deposit. These broken dendrites are postulated to result in grain multiplication when cooling in the deposit. Such a mechanism does not explain why the finished ingot contains these beneficial microstructural features already outlined above. Needless to say the debate that Grant outlines in his review regarding the microstructural evolution during spray forming has not abated or been satisfactorily outlined yet.

This contribution aims to provide a new explanation for the fine microstructural and rapid solidification features evident in spray formed products. Using a single fluid atomization technique, Impulse Atomisation (IA), the microstructure of Al-Cu and Al-Fe alloy powders will be examined and quantified. A spray forming unit based on IA will be introduced where spray formed strip of Al-Fe was produced in an experimental set-up. The microsctructure of the strip was quantified and compared to that of the powder. These results are used to formulate a new mechanism for the solidification path of a spray deposit. It will be termed the *slushy balloon model*.

2 Experimental

Impulse Atomization (IA) was developed at the Advanced Materials and Processing Laboratory (AMPL) at the University of Alberta, Canada. This technique has been used for making metal powders, spray deposits, metal-matrix composites and spray refining of pig iron. Basically, this technique takes advantage of the fact that a liquid jet emanating from a capillary can be destabilized when disturbed by a particular shock wave frequency. IA has successfully atomized metallic materials like aluminum, zinc, copper, cobalt, nickel, and their alloys as well as steel.

Dept of Chemical and Materials Engineering, 276B Chemical-Materials Engineering, University of Alberta, Edmonton, Alberta, CANADA T6G 2G6

Correspondence author: H. Henein, Dept of Chemical and Materials Engineering, 276B Chemical-Materials Engineering, University of Alberta, Edmonton, Alberta, CANADA T6G 2G6
E-mail: hani.henein@ualberta.ca

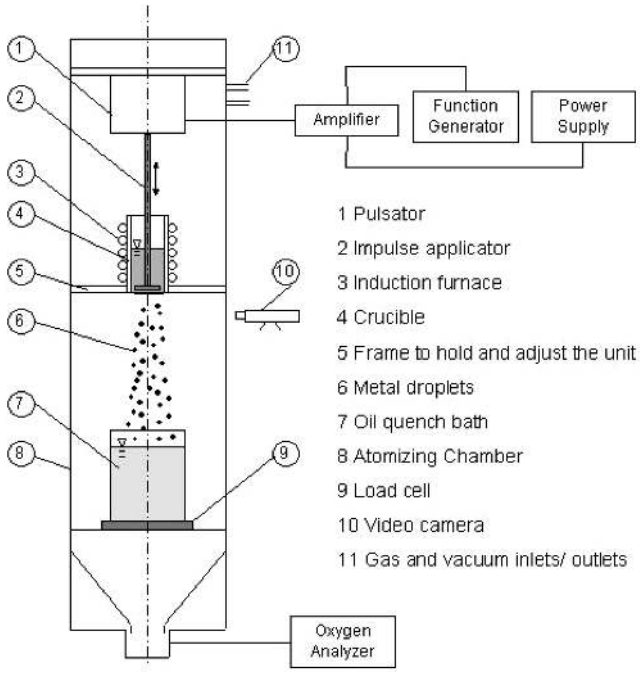

Figure 1. Schematic diagram of the IA apparatus for the generation of powder fully solidified in the gas during free fall.

The IA apparatus for powder generation is schematically shown in *Figure 1*. The impulse unit includes an alumina plunger attached to a 100 Hz pulsator which impulses the molten metal through a nozzle (a series of capillaries) on the bottom of the crucible. The impulses generate discontinuous streams of molten metal, which emanate from the nozzle. The streams result in ligands, which in turn break up into droplets. The droplets fall in a static gas atmosphere and solidify as spherical particles [2]. A thermocouple is immersed in the crucible to record melt temperature near the atomizing nozzle. Pilot scale tests have been carried out with IA for the successful atomization of zinc through up to 400 orifices operating for 3 continuous hours.

Table 1. IA run conditions for atomized Al-0.61 wt% Fe alloy powder

Run Number	Sample name	Gas	d_{50} [μm]	geo σ [–]
030108 I	I	N_2	392	1.37
030108 K	K	He	435	1.42

For the generation of spray formed strip, an experimental unit based on the IA technique was constructed. A schematic is shown in *Figure 2*. The generation of droplets is the same as described above. A copper substrate is placed about 0.4 m below the point of generation of the spray [3]. The substrate is moved laterally at a specified speed in order to collect the droplets under a nitrogen gas atmosphere. A thermocouple is placed at the location of deposition of the spray with the deposit. By controlling the number of orifices in the crucible for atomization, the speed of the movement of the substrate and the distance the substrate is located away from the crucible, the size of the deposit may be controlled. *Figure 3* presents a typical macro image of the strip analysed in this work, as well as a trace of the thermocouple measurement as a function of time, indicating that thermal steady state was achieved in the experiment.

The objective of the present contribution is to use IA as a research tool in understanding the mechanism of microstructure evolution during the solidification of spray formed ingots. Al-0.6 wt%Fe alloy was used for both the powder and spray formed deposited strip experiments under the effect of different cooling conditions, e.g. helium and nitrogen are used as cooling gases. Quantitative microstructural analysis will be reported for these alloys.

2.1 Impulse atomisation runs

All the powder samples in this paper were atomized under conditions listed in *Table 1* and the run conditions for the Al-0.61 wt% Fe alloy strip are given in *Table 2*. For this work, alloys were melted in a graphite crucible having a melt capacity of about 0.5 l

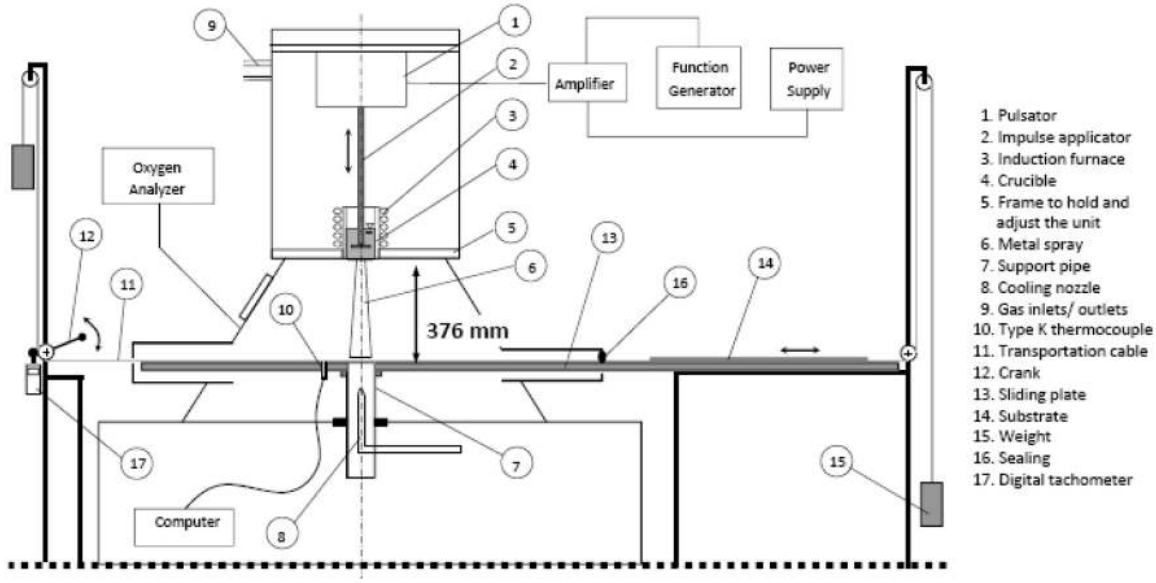

Figure 2. Schematic diagram of the IA apparatus for the generation of strip.

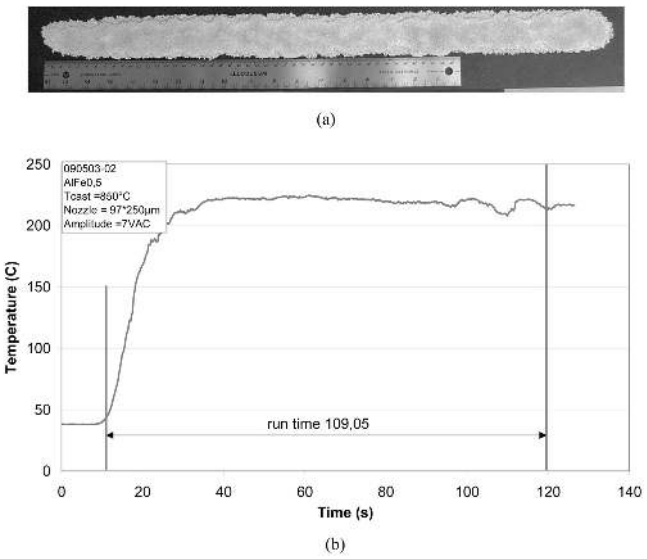

Figure 3. (a) Macro-image of typical strip produced and listed in Table 2; (b) temperature measurement below the copper substrate where the Al-0.61Fe spray falls onto the substrate.

Table 2. IA run conditions for atomized Al-0.61 wt% Fe alloy strip

Run Number		090503-02	082603-03	082603-05
Run time	(s)	109	71	44
deposit mass	(g)	198	136	73
mass flow	(g/s)	1.82	1.91	1.66
substrate feed	(mm/s)	5.78	8.07	7.69
# layers		1	1	1
deposit length	(mm)	630	575	335

using an induction furnace. The alloys were prepared from granules of 99.9 wt%Al and wires of 99.90 wt%Fe. Other experimental conditions were a superheat of approximately 200 K above the nominal liquidus point, 97 holes in the nozzle plate having orifice diameters of 250 µm. The oxygen in the gas atmosphere was between 300 and 400 ppm.

Chemical analysis on the atomized powders was performed following ASTM E1097-97 (modified) and E1479-99. Impurities less than 100 ppm were not determined in the powder samples.

The IA powders produced were sieved according to the Metal Powder Industries Federation Standard 05. The d_{50} and log-normal standard deviation ($\sigma = d_{84}/d_{50}$) are reported in Table 1. The values of d_{50} and σ for the samples of each run have been calculated using the measured sieve analysis and the calculation method of Bokyo and Henein [3].

2.2 Metallography and microscopy

The powders and strip were cold mounted in epoxy and polished with as fine a media as 0.05 µm alumina polishing suspension. The polished samples were then etched using Keller's solution.

An optical microscope Olympus PME 3 with an attached video camera was used to take photomicrographs of samples of each size range. The characteristic length of cell spacing, λ, i. e. the distance between two consecutive cellular/dendritic α-Al centers, is to be used as the microstructure characterization. This distance gives also a very close value of the cell size or diameter. In the observation of powders, ten micrographs of each average particle size were taken. The software "imageJ" was used for the analysis of the micrographs. For each micrograph, five horizontal lines were drawn across the particle microstructure. Then, the number of cell intercepts, c, was counted manually for a line of known length, l. Most of the cell spacings, λ, were therefore calculated using 50 lines to get a statically meaningful value. The cell spacing, λ, is then determined using the following equation (1):

$$\lambda = \frac{l}{c} \tag{1}$$

Finer observations of the microstructure were carried out using a JEOL 6301F Field Emission Scanning Electron Microscope (FESEM). Energy dispersive X-ray analysis (EDAX) was used to get semi quantitative microanalysis of the iron content in specific spots of the observed area.

Additional quantification of the microstructure was also carried out. The fraction of eutectic was measured using the following procedure. Regions of interest in micrographs from optical microscopy were chosen. Then each picture was processed using the "color to greyscale" and "threshold" functions of the software ImageTool (ImageTool version 3.00, developed by the University of Texas Health Science Centre in San Antonio, Texas, US). The processed picture was then analysed using the "count black/white pixels" function. The black pixels were assumed to be representative of areas of eutectic. This assumes that there is negligible volume fraction of solidification shrinkage in the powder particles. Finally, the surface% of eutectic value obtained is taken to be equal to the volume% of eutectic value.[4]

3 Results

3.1 Observed microstructures

The microstructures of Al-0.61Fe powder samples observed for different particle sizes showed very similar features. *Figure 4* shows the typical cell microstructure and focuses on the cell boundary, which show a typical lamellar structure: regular structure made of dark and light more or less parallel stripes. The scale and the cell spacing change when the particle size changes, but the microstructure does not. A fully dendritic microstructure, defined by light cells, surrounded by dark boundaries, is visible. Previous work has shown that the structure of Al-0.61Fe is composed of primary α-Al and a eutectic [5]. *Figure 5* shows a typical microstructure at the mid-thickness of the 3 mm strip. Visible is the primary α-Al phase surrounded by eutectic.

3.2 Cell Spacing and Eutectic Fraction

The cell spacing for the atomised powder is shown in *Figure 6* for experiments carried out in He and in N_2 gases. As expected the powders atomised in Helium is much finer in structure than those atomised in nitrogen gas. The cell spacing ranges between about 9 and 18 µm for powders sizes from 165 to 925 µm in size atomised in nitrogen gas.

The results of the measured (surface%) of eutectic for samples K and I (Al-0.61Fe), converted in volume% are compared to the

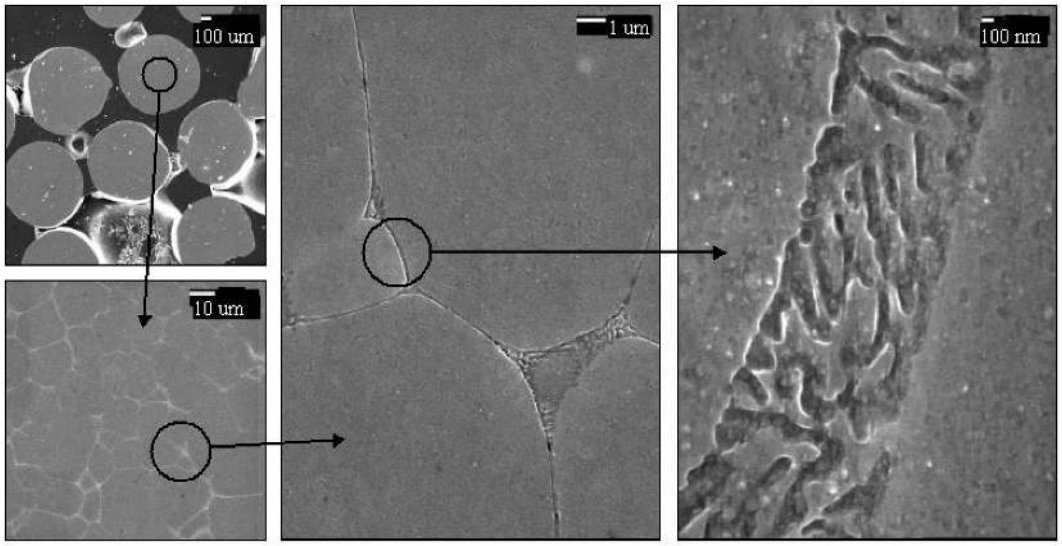

Figure 4. FESEM micrographs of the typical microstructure found in sample I (Al-0.61Fe, N_2), average particle size of 925 μm.

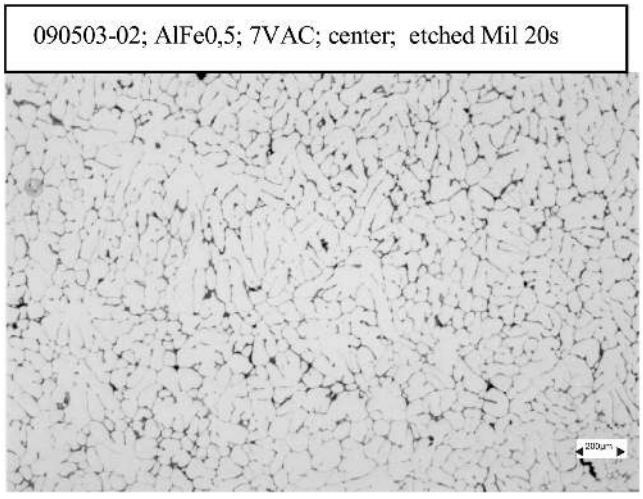

Figure 5. Microstructure of strip near mid-thickness of the strip showing a much coarser primary α-Al than in powder and eutectic between the primary phase. Note that the micron marker indicates a spacing of 200 μm.

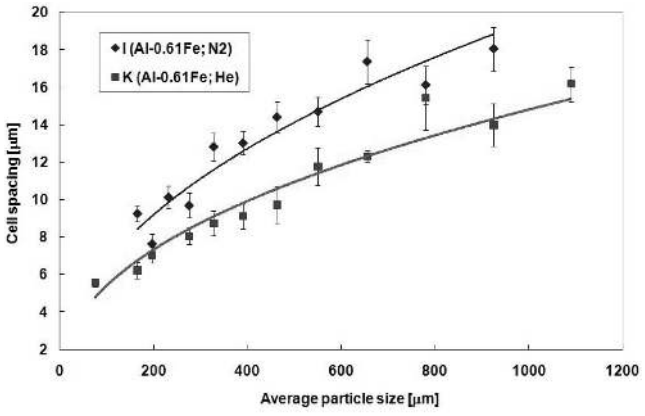

Figure 6. Cell spacing versus powder size for Al-0.61Fe atomised in He and N_2. [5]

Table 3. Cell spacing and Eutectic fraction in Mid-thickness Strip Samples

Run Number	(–)	090503-02	082603-03	082603-05
Average cell spacing	(μm)	44.2	42.9	41.2
Standard deviation	(μm)	6.2	6.7	2.6
Percent eutectic		15.7	13.7	15.7
Standard deviation		3.1	2.6	3.1

volume% of eutectic that would have formed under either equilibrium conditions or Scheil-Gulliver solidification, *Figure 7*. The volume percent of eutectic that would form from equilibrium calculated from the Al-$Al_{13}Fe_4$ phase diagram is 32.4 wt% of eutectic converted to volume percent [5].

The experimental results for samples I and K mostly lie between about 17 and 20 vol% eutectic. Because of the experimental error in measurements, it is not possible to note a difference between the trend in eutectic fraction with particle size using either nitrogen or helium.

From Figure 7, there is a big difference between the values of the volume% eutectic given by measurements (helium or nitrogen), and those calculated based on the equilibrium phase diagram and Scheil-Gulliver. The experimental measurements are all well below the calculated values from the equilibrium phase diagram and Scheil-Gulliver. This will be discussed later in this work.

Table 3 lists the cell spacing and percent eutectic results for the three strip samples reported. Despite the standard deviation of the results, it can be clearly seen that the cell spacings are nearly 2 to 4 times larger than those for powders (compare results in *Table 3* and Figure 6); while the eutectic fraction is nearly the same, Table 3 and Figure 7. Also note that the eutectic fraction in the strip is considerably away from either equilibrium values or

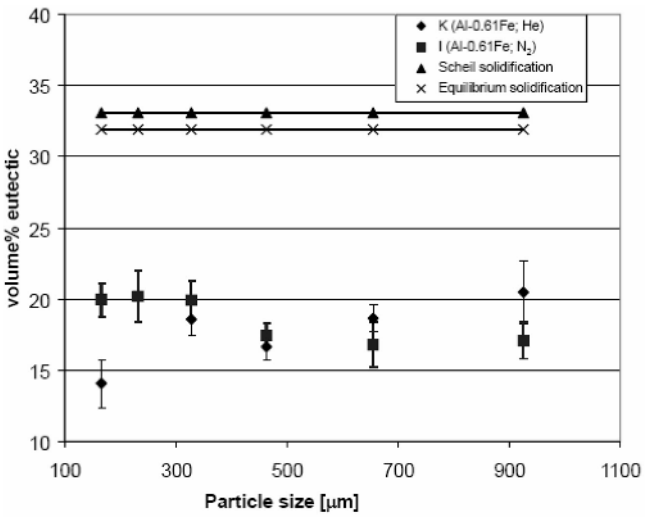

Figure 7. Volume fraction of eutectic for powders atomised in helium and nitrogen. Also shown are the equilibrium fraction of eutectic as well as the fraction that would form under Scheil-Gulliver conditions [5].

Shiel-Gulliver calculation shown in Figure 7. This will be discussed again in the following section of this work.

4 Discussion

A recent paper by Ellendt et al [6] compared spray deposition using IA with Gas Atomisation (GA). In that work Cu-6Sn was atomised and spray deposited in the form of an ingot. It was found that while the porosity of the spray formed ingot was nearly the same, the cooling rate of the gas atomised ingot was significantly larger than that predicted for the IA ingot. The cooling rate of the IA ingot ranged between 2.5 and 1 K/s. A comparison of the grain sizes between GA and IA ingots revealed that the grain size of the GA ingot was significantly smaller than that of the IA ingot (Figure 8). Figure 9 shows a comparison of the hardness of both ingots as well as the porosity. The range of porosity and hardness for the GA spray formed ingot is outlined using dashed lines. The points represent measurements on the IA ingot. Clearly the porosity is nearly the same for both IA and GA. However, the hardness of the IA ingot is higher than that for the GA ingot. This is occurring despite the fact that the grain size of the GA ingot is smaller than that for the IA ingot. This result is very puzzling and can only be explained if there is a higher extended solubility of Sn in the Cu ingot for the IA ingot than for the GA ingot.

Using levitated droplets of a range of Al-Cu alloys, Gandin et al. [7] measured the temperature of the cooled droplets. They report on a microsegregation model that accounts for the coupled growth of eutectic. It is clear from that work that eutectic undercooling was quite prevalent in the solidification of the droplets. When those values of eutectic undercooling were used in a microsgregation model of rapidly solidified Al-Cu alloys atomised using IA, excellent agreement was achieved for the eutectic fraction of all droplets measured and predicted.[8]

The same departure from equilibrium and Scheil-Gulliver prediction was observed in the Al-Fe alloy, Figure 7, [5]. As discussed by the authors, the solidification does not follow the equilibrium path and undercooling of the Al-Fe intermetallic is taking place (i. e. eutectic undercooling). That is, there is a greater amount of primary phase than is given by the equilibrium phase diagram. Hence eutectic undercooling plays a significant role in the solidification of these binary eutectic alloys.

A discussion comparing the heat transfer conditions in both Impulse Atomization to produce powder and Impulse Atomization to produce spray formed strip is in order. A very detailed analysis of the heat transfer mechanism for cooling and solidifying droplets was presented by Wiskel et al. [9, 10]. In this work two scales of the primary α aluminum was reported. The coarser was shown to be solidified primary phase of aluminum which occurred while the droplets fell through the gas phase. The much finer structure of primary ά phase aluminum in the alloy powder that was also reported by Olsen et al. [11] is due to a fraction of liquid in the droplet that remains unsolidified in the gas while the droplet is falling, but solidifies in the quench bath. A series of analyses on various sized droplets verified the heat transfer model for the cooling of droplets in Impulse Atomization and shown that all droplets less than 1 mm of aluminum alloys would be fully solid by falling through the gas a distance of 4 m where the quench bath is commonly placed a the bottom of

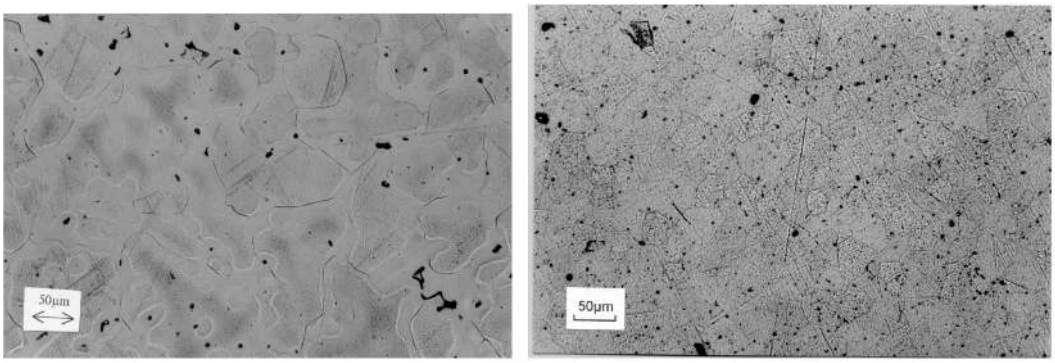

Figure 8. (a) Optical micrographs of IA Cu-6Sn spray formed ingot taken 3mm above the bottom, and (b) Optical micrograph of GA Cu-6Sn spray formed ingot having a billet diameter of 100mm, billet height 140mm, sample taken 40 mm above the bottom [6].

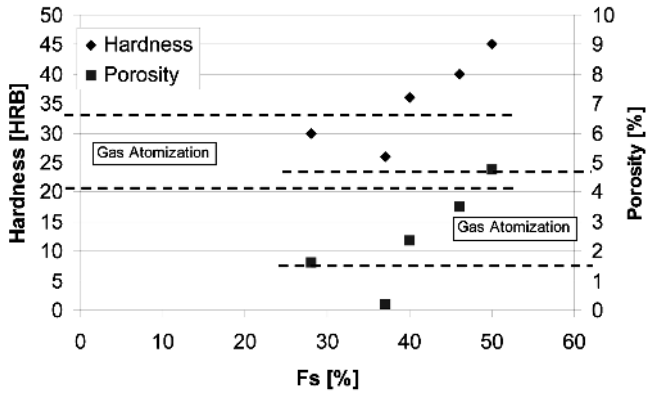

Figure 9. Results of hardness and porosity of spray formed Cu-6Sn alloy as a function of the fraction of solid of droplets depositing on the spray formed ingot for both IA and GA [6].

the atomizing tower. Thus, the main mechanism of heat loss of the solidified droplets is forced convection to the gas.

For the spray forming of strip, the situation for heat transfer loss from the deposit is more complicated. This discussion will be restricted to periods of operation of spray forming when under steady state. That is when a relatively constant temperature is measured at the bottom of the 1.27 mm thick copper substrate as shown in Figure 3b. This steady state period is from about 40 to 100 seconds. At a position of 0.4m from the nozzle plate, the droplet atomized through a nozzle having 97 orifices each with 250 μm in diameter and an atomizing temperature of 850 °C, would result in greater than 50% of the atomized droplet arriving at the substrate semi-solid. This is based on the fact that Impulse Atomization provides typically droplets of a geometric size distribution of 1.4 and that the D50 for this experiment would be estimated to be 350 μm [2]. Those droplets in direct contact with the copper substrate would clearly have a quench type of structure. As more semi-solid droplets land on the deposit, the heat loss from these droplets will be through the deposit and the now heated copper substrate as well as through the surface of the deposit to the gas atmosphere. At mid-thickness of the deposit (about 1.5 mm), the structure apparent in the deposit shown in Figure 5 is clearly that of a very coarse structure, indicative of a very slow cooling rate. Clearly, the effect of cooling of the copper substrate is not evident at the mid-thickness of the deposit. If any of the droplets were fully solid in the deposit, where cell spacing measurements were taken, a very fine structure similar to that measured in the droplets would have been observed. No such fine structure is seen in Figure 5. In fact, the structure is clearly quite homogeneous and coarser than is the case for droplets solidified fully in the gas phase. Measurements of cell spacing near the copper substrate only indicated an average of about 10 μm less than that measured in mid-thickness and 3 times higher than those measured for powders (Figure 6). Hence the cooling rate of the deposit is clearly much lower than that for the powders. This is further confirmed by the model predictions of cooling rate of a spray deposit in Impulse Atomization reported by Ellendt et al [6]. In this work a mathematical model of the cooling at the mid section of a spray formed Cu-6Sn Impulse ingot was developed. It was reported that even for a substrate thickness of 1mm, the maximum cooling rate of the deposit adjacent to the substrate at the mid-section is 2.5 °C/s. This is two orders of magnitude smaller than the coarsest droplet size (1 mm) cooling in a gas in Impulse Atomization. [8–10] It was concluded that the main mechanism of heat loss from an IA spray formed ingot is that of very mild convection at the top surface of the ingot.

Despite the difference in cooling rate between powders and spray formed strip (at mid-thickness), the similarity of eutectic fraction between strip and droplet seems quite surprising. This can only suggest that the same eutectic undercooling mechanism is taking place in the strip as is occurring in the droplets. In order for that to occur then there cannot be any liquid merging between adjacent droplets in the strip.

Consider that in atomization there is always a small but finite amount of oxygen present in the atomizing chamber. The microstructure evolution in IA spray forming is therefore postulated to be as follows. When droplets are atomized, they will be covered by a nano thick coating of oxide. In the case of Al-Fe alloys, this would be alumina. As the droplet falls in the tower, primary phase undercooling occurs, followed by recalescense and subsequent growth of the primary α-Al solid. When the droplet lands on the deposit it still has a significant amount of liquid, about 30 to 50% depending on size, superheat and free fall distance between the nozzle and the deposit. In the deposit the droplet will deform but for most of the droplets, the oxide coating will likely not break. Thus in the deposit, a droplet having an oxide coating will be termed the ‚droplet region' in the strip. As solidification continues in the deposit, the ‚droplet regions' will solidify independent of solute in adjacent ‚droplet regions'. When the deposit further cools, each ‚droplet region' in the deposit must nucleate its own second phase. Hence, one achieves eutectic undercooling of the same order as occurs in droplet solidification.

This mechanism can be described in terms of a falling balloon that is filled with slush. When the balloon lands onto a substrate with other balloons surrounding it and further cools, the solid forming in each balloon will form independent of the one in an adjacent balloon. Hence each ‚droplet region', i. e. balloon, solidifies in the deposit independent of the solute segregation occurring in an adjacent ‚droplet region'.

In GA, droplets are moving very fast with the atomising gas. Even though they will land on the deposit with more force that in IA, because of their smaller size then in IA, most of the oxide coatings will not be expected to break. This will result in extended solubility, metastable phases, or extended solubility in each droplet region. So the *slushy balloon model* will be expected to be active in spray forming using GA. Its extent will vary on a range of parameters which clearly include the alloy composition.

5 Conclusions

The microstructure evolution in spray formed deposits is governed by a range of coupled phenomena. The first of which is the formation of an oxide coating on the droplets. This coating remains intact for many droplets as primary phase undercooling occurs followed by droplet recalescence, droplet impact with the substrate or deposit, and the undercooling of the eutectic. This sequence of events results in a highly refined structure with

extended solute solubility, lower fraction of eutectic or metastable phases in the deposit.

Acknowledgements

The author wishes to acknowledge the contributions of J. Knabe, R.-R. Schmidt, T. Lewandowski, J. Chen, V. Buchould, A. Rosensctock, and A. Edwards in making many of the measurements presented in this work. Furthermore, the financial assistance of NSERC and the Canadian Space Agengy is gratefully acknowledged.

6 References

[1] P.S. Grant, *Progress in Materials Science* **1995**, *39*, 497.

[2] H. Henein, *Materials Science and Engineering A – Structural Material Properties, Microstructure and Processing* **2002**, *326*, 92.

[3] C. M. Boyko, H. Henein, Computer Software in Chemical and Extractive Metallurgy: 2nd International Symposium, *32nd Conference of Metallurgists*, Met. Soc of CIM, Montreal, **1993**, 289.

[4] A. Prasad, H. Henein, E. Maire, Ch.-A. Gandin, *Metall. Mater. Trans., A* **2006**, *37*, 249.

[5] H. Henein, V. Buchoud, R.-R. Schmidt, C. Watt, D. Malahof, C.-A. Gandin, G. Lesoult, V. Uhlenwinkel, *Cdn Metallurgical Quarterly* **2009**, *in press.*

[6] N. Ellendt, R. Schmidt, J. Knabe, H. Henein, V. Uhlenwinkel, *Materials Science and Engineering A* **2004**, *383*, 107.

[7] C.-A. Gandin, S. Mosbah, Th. Volkmann, D. Herlach, *Acta Materalia* **2008**, *56*, 3023.

[8] A. Prasad, S. Mosbah, H. Henein, C.-A. Gandin, *ISIJ International* **2009**, *49*, 992.

[9] J. B. Wiskel, H. Henein, E. Maire, *Canadian Metallurgical Quarterly* **2002**, *41*, 97.

[10] J. B. Wiskel, K. Navel, H. Henein, E. Maire, *Canadian Metallurgical Quartely* **2002**, *41*, 193.

[11] K. Olsen, G. Sterzik, H. Henein, *International Journal of Powder Metallurg* **2001**, *37*, 55.

Received in final form: May 12th 2010 T 642

